

The horn, the hadron mass spectrum and the QCD phase diagram - the statistical model of hadron production in central nucleus-nucleus collisions

A. Andronic^a, P. Braun-Munzinger^{a,b,c,d}, and J. Stachel^e

^aGSI Helmholtzzentrum für Schwerionenforschung, D-64291 Darmstadt, Germany

^bExtreMe Matter Institute EMMI, D-64291 Darmstadt, Germany

^cTechnical University Darmstadt, D-64289 Darmstadt, Germany

^dFIAS, J.W Goethe University, D-60438 Frankfurt, Germany

^ePhysikalisches Institut der Universität Heidelberg, D-69120 Heidelberg, Germany

One of the major goals of ultrarelativistic nuclear collision studies is to obtain information on the QCD phase diagram [1]. A promising approach is the investigation of hadron production. Hadron yields measured in central heavy ion collisions from AGS up to RHIC energies can be described very well (see [5] and refs. therein) within a hadro-chemical equilibrium model. In our approach the only parameters are the chemical freeze-out temperature T , the baryo-chemical potential μ_b and the fireball volume V (for a review see [2]).

The main result of these investigations was that the extracted temperature values rise rather sharply from low energies on towards $\sqrt{s_{NN}} \simeq 10$ GeV and reach afterwards constant values near $T=160$ MeV, while the baryochemical potential decreases smoothly as a function of energy. The limiting temperature [3] behavior suggests a connection to the phase boundary and it was, indeed, argued [4] that the quark-hadron phase transition drives the equilibration dynamically, at least for SPS energies and above. Considering also the results obtained for elementary collisions, where similar analyses of hadron multiplicities, albeit with several additional, non-statistical parameters (see [5,6] and refs. therein), yield also temperature values in the range of 160 MeV, alternative interpretations were put forward. These include conjectures that the thermodynamical state is not reached by dynamical equilibration among constituents but rather is a generic fingerprint of hadronization [7,8], or is a feature of the excited QCD vacuum [9].

While in general all hadron yields are described rather quantitatively, a notable exception was up-to-now the energy dependence of the K^+/π^+ ratio which exhibits a rather marked maximum, “the horn” [10], near $\sqrt{s_{NN}} \simeq 10$ GeV [11]. Predicted first within a model of quark-gluon plasma (QGP) formation [10], the existence of such a maximum was also predicted [12] within the framework of the statistical model, but the observed rather sharp structure could not be reproduced [13] (see also the discussion in [11]). As a consequence, the horn structure is taken in [11] as experimental evidence for the onset of deconfinement and QGP formation, and as support for the predictions of [10]. We have

recently shown [14] that, employing an improved hadronic mass spectrum, in which the σ meson and many higher-lying resonances are included, leads to a sharpening the structure in the K^+/π^+ ratio, as will be shown below.

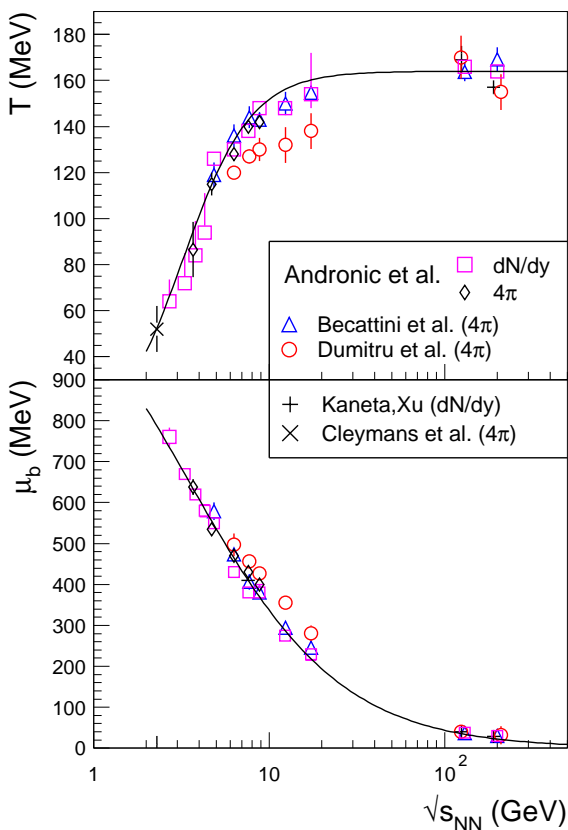


Figure 1. The energy dependence of the temperature and baryon chemical potential at chemical freeze-out. The results of the new fits [14] are compared to the values obtained in our earlier study [13]. The lines are parametrizations for T and μ_b (see text).

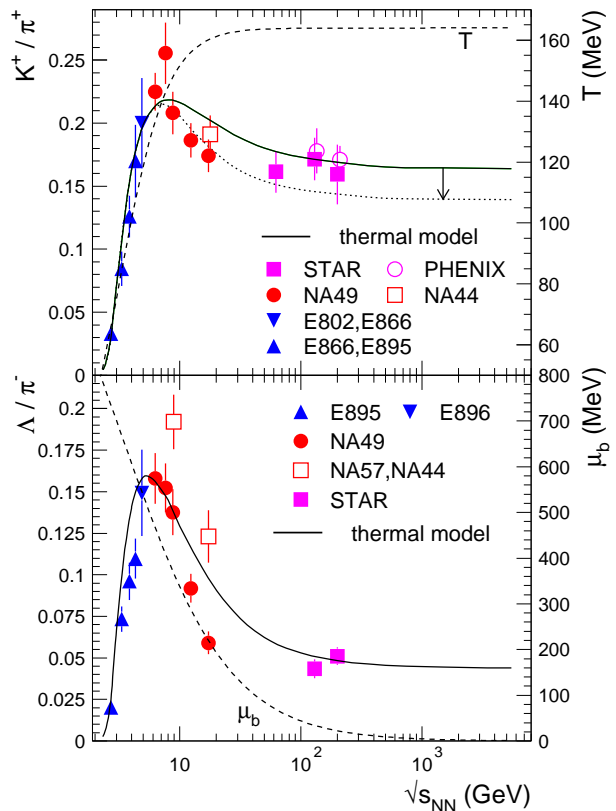


Figure 2. Energy dependence of the relative production ratios K^+/π^+ and Λ/π^- . With the dotted line we show for the K^+/π^+ ratio an estimate of the effect of higher mass resonances. The dashed lines show the energy dependence of T and μ_b .

In Fig. 1 we present the energy dependence of T and μ_b in comparison to results of other similar analyses [15,16,17,18]. In [18] the strangeness suppression factor γ_s is an additional fit parameter; in [17] an inhomogeneous freeze-out scenario is modeled with spreads in T and μ_b as extra fit parameters; the approach of [19], employing a full set of non-equilibrium fit parameters, leads to rather different results compared to those shown here. We have parametrized our values of T and μ_b as a function of $\sqrt{s_{NN}}$ with the following expressions:

$$T = T_{lim} \frac{1}{1 + \exp(2.60 - \ln(\sqrt{s_{NN}}(\text{GeV}))/0.45)}, \quad \mu_b[\text{MeV}] = \frac{1303}{1 + 0.286\sqrt{s_{NN}}(\text{GeV})} \quad (1)$$

with the "limiting" temperature $T_{lim}=164$ MeV.

We employ the above parametrizations of T and μ_b to investigate the energy dependence of the production yields of K^+ and Λ hadrons relative to pions, shown in Fig. 2. The K^+/π^+ ratio shows a rather pronounced maximum at a beam energy of 30 AGeV [11], and the data are well reproduced by the model calculations. In the thermal model this maximum occurs naturally at $\sqrt{s_{NN}} \simeq 8$ GeV [12]. It is due to the counteracting effects of the steep rise and saturation of T and the strong monotonous decrease in μ_b . The competing effects are most prominently reflected in the energy dependence of the Λ hyperon to pion ratio (lower panel of Fig. 2), which shows a pronounced maximum at $\sqrt{s_{NN}} \simeq 5$ GeV. This is reflected in the K^+/π^+ ratio somewhat less directly; it appears mainly as a consequence of strangeness neutrality, assumed in our calculations.

The model describes the K^+/π^+ data very well over the full energy range, as a consequence of the inclusion in the code of the high-mass resonances and of the σ meson, while our earlier calculations [13] were overpredicting the SPS data. At RHIC energies, the quality of the present fits is essentially unchanged compared to [13], as also the data have changed somewhat. The model also describes accurately the Λ/π^- measurements as well as those for other hyperons [14].

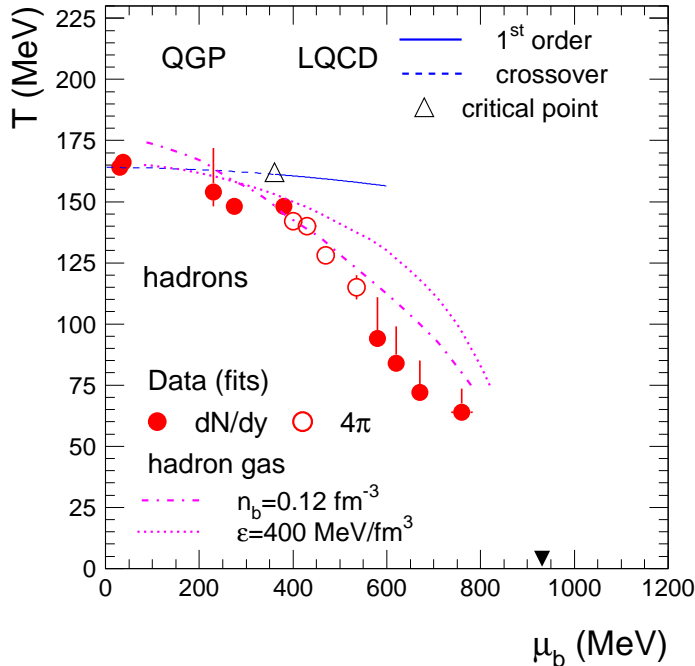


Figure 3. The phase diagram of strongly interacting matter. The points represent the results of the thermal fits. For the SPS beam energy of 40 AGeV ($\mu_b \simeq 400$ MeV) we show both midrapidity (dN/dy) and full phase space (4π) fit results. The phase boundary and critical point from lattice QCD (LQCD) calculations [20] is shown together with freeze-out curves for a hadron gas at constant baryon density (baryons and anti-baryons) and energy density. The full triangle indicates the location of ground state nuclear matter (atomic nuclei).

In Fig. 3 we show the result of our fits in the phase diagram of strongly interacting matter (for a recent review see [22]). Our results strongly imply that hadronic observables near and above the horn structure at a beam energy of 30-40 AGeV ($\mu_b \simeq 400$ MeV), coinciding with the approach to saturation in T , provide a link to the QCD phase transition. Open questions are whether the chemical freeze-out curve for larger values of μ_b actually traces the QCD phase boundary or whether chemical freeze-out in this energy range is influenced by exotic new phases such as have been predicted in [21].

In summary, our recent results [14] demonstrate that by inclusion of the σ meson and

many higher mass resonances into the resonance spectrum employed in the statistical model calculations an improved description is obtained of hadron production in central nucleus-nucleus collisions at ultra-relativistic energies. A dramatic improvement is visible for the K^+/π^+ ratio, which is now well described at all energies. The “horn” finds herewith a natural explanation which is, however, deeply rooted in and connected to detailed features of the hadronic mass spectrum which leads to a limiting temperature and contains the QCD phase transition [3].

We acknowledge the support from the Alliance Program of the Helmholtz-Gemeinschaft.

REFERENCES

1. P. Braun-Munzinger, J. Wambach, Rev. Mod. Phys. **81** (2009) 1031 [arXiv:0801.4256].
2. P. Braun-Munzinger, K. Redlich, and J. Stachel, nucl-th/0304013, invited review in Quark Gluon Plasma 3, eds. R.C. Hwa and X.N. Wang, (World Scientific Publishing, 2004).
3. R. Hagedorn, CERN-TH-4100/85 (1985).
4. P. Braun-Munzinger, J. Stachel, C. Wetterich, Phys. Lett. B **596** (2004) 61 [arXiv:nucl-th/0311005].
5. A. Andronic, F. Beutler, P. Braun-Munzinger, K. Redlich, J. Stachel, Phys. Lett. B **675** (2009) 312 [arXiv:0804.4132].
6. F. Becattini, P. Castorina, J. Manninen, H. Satz, Eur. Phys. J. C **56** (2008) 493 [arXiv:0805.0964].
7. R. Stock, Phys. Lett. B **465** (1999) 277 [hep-ph/9905247].
8. U. Heinz, Nucl. Phys. A **685** (2001) 414 [hep-ph/0009170].
9. P. Castorina, D. Kharzeev, H. Satz, Eur. Phys. J. C **52** (2007) 187 [arXiv:0704.1426].
10. M. Gaździcki, M.I. Gorenstein, Acta Phys. Polon. B **30** (1999) 2705 [hep-ph/9803462].
11. C. Alt et al. (NA49), Phys. Rev. C **77** (2008) 024903 [arXiv:0710.0118].
12. P. Braun-Munzinger, J. Cleymans, H. Oeschler, K. Redlich, Nucl. Phys. A **697** (2002) 902 [hep-ph/0106066].
13. A. Andronic, P. Braun-Munzinger, J. Stachel, Nucl. Phys. A **772** (2006) 167 [nucl-th/0511071].
14. A. Andronic, P. Braun-Munzinger, J. Stachel, Phys. Lett. B **673** (2009) 142 [arXiv:0812.1186], Erratum: ibid. B **678** (2009) 516; Acta Phys. Pol. **40** (2009) 1005 [arXiv:0901.2909].
15. J. Cleymans and K. Redlich, Phys. Rev. C **60** (1999) 054908 [nucl-th/9903063].
16. N. Xu and M. Kaneta, Nucl. Phys. A **698** (2002) 306c. the model of
17. A. Dumitru, L. Portugal, D. Zschesche, Phys. Rev. C **73** (2006) 024902 [nucl-th/0511084].
18. F. Becattini, M. Gaździcki, J. Manninen, Phys. Rev. C **73** (2006) 044905 [hep-ph/0511092], J. Manninen, F. Becattini, Phys. Rev. C **78** (2008) 054901 [arXiv:0806.4100].
19. J. Letessier, J. Rafelski, Eur. Phys. J. A **35** (2008) 221 [nucl-th/0504028].
20. Z. Fodor, S.D. Katz, JHEP **404** (2004) 50 [hep-lat/0402006].
21. L. McLerran and R. Pisarski, Nucl. Phys. A **796** (2007) 83 [arXiv:0706.2191].
22. R. Stock, arXiv:0909.0601.